Phase Equilibria of the Mg-Y-Zn System at 500 °C in the Mg-Rich Region

Honghui Xu[1] · Hai-Lin Chen[2] · Tao Zhou[1]

Abstract The Mg-rich phase equilibria of the Mg-Y-Zn system at 500 °C were investigated with equilibrated alloys, by means of electron probe microanalysis and x-ray diffraction. A partial isothermal section of < 34 at.% Y and < 50 at.% Zn was constructed and an extended section of < 50 at.% Y was produced by integrating our previous results in the Zn-rich region. Following the previous finding of seven ternary phases (τ_1 to τ_7) in the Zn-rich region, seven more ternary phases (τ_8 to τ_{14}) were found in the Mg-rich region in the present work. With the systematic composition measurement and XRD analysis, six of them (τ_8 to τ_{13}) were determined to be the so-called LPSO phases. They are very close to one another in composition and located approximately along the line of Y/Zn ratio = 4/ 3. τ_8 is believed to be X-$Mg_{12}YZn$ (14H), τ_9 to be $Mg_{10}ZnY$ (18R) and τ_{13} to be 10H.

Keywords electron probe microanalysis (EPMA) · long-period stacking ordered (LPSO) phase · Mg-Rare earth alloys · phase diagrams · x-ray diffraction

1 Introduction

The long-period stacking ordered (LPSO) structures[1–7] and quasicrystals[8] in the Mg-Y-Zn alloys have received intensive attention world-wide for the past decades not only from materials scientists but also from physicists. So far, four types of LPSO structures (i.e. 10H, 14H, 18R and 24R) have been found in the Mg-Y-Zn alloys.[2,3,5,6] Among them, 18R and 14H are the most commonly observed LPSO structures.[5,7] The 18R phase is generally believed to form during solidification of the Mg-Y-Zn alloys while the 14H phase to precipitate during subsequent heat treatments.[4,5] Nevertheless, Matsuda et al.[6] suggested that the four types of LPSO structures (18R, 14H, 10H and 24R) had been simultaneously observed in the rapidly solidified $Mg_{97}Zn_1Y_2$ alloy. In addition, it is worth mentioning that the evaluated compositions for 14H and especially for 18R by different groups of researchers are significantly different, as illustrated by Egusa and Abe.[7] Up to now, the total number of stable LPSO phases, their stability and composition ranges still remain undetermined, mainly due to their tiny structural differences and large discrepancy among the reported compositions for the same structures by different groups of researchers.

Knowledge of the phase equilibria in the Mg-Y-Zn system is of fundamental importance for advancing the development of the Mg-Y-Zn based alloys. In our previous work,[9] the phase equilibria at 500 °C in the Zn-rich region were investigated in detail and seven ternary phases (τ_1 to τ_7) found, as shown in Fig. 1. The present work aims at the determination of the phase equilibria at 500 °C in the Mg-rich region involving the LPSO phases. This work is carried out within the framework of a long-term project for investigating the phase equilibria in the Mg-RE-Zn systems (RE = Rare Earth).[9,10]

✉ Honghui Xu
  hhxu@csu.edu.cn

1 State Key Laboratory of Powder Metallurgy, Central South University, Changsha 410083, People's Republic of China

2 Thermo-Calc Software AB, Råsundavägen 18, 16967 Solna, Stockholm, Sweden
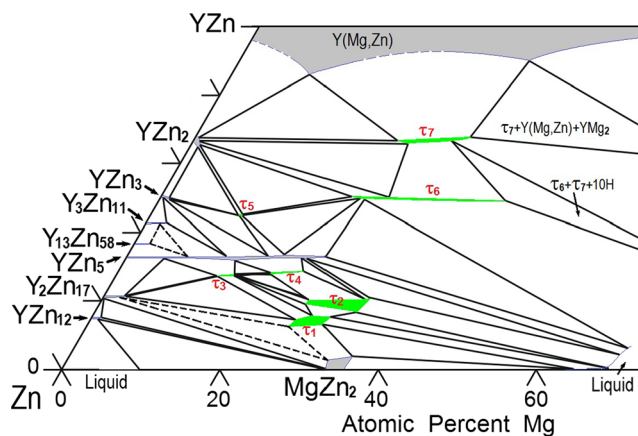
Fig. 1 Isothermal section at 500 °C in the Zn-rich range reported by Zhou et al.[9]

2 Experimental Procedures

Sixteen different Mg-Y-Zn alloys were prepared with high-purity Magnesium (99.99 wt.%), Zinc (99.999 wt.%) and yttrium (99.9 wt.%). Yttrium was cut into small blocks and kept ready in acetone for use. The oxide layers on the surfaces of the yttrium, magnesium and zinc blocks were mechanically removed before weighting. The accurately weighed materials of the Zn, Mg and Y blocks were cleaned with acetone and sealed in the Ta crucibles, which were then individually sealed in quartz tubes. The quartz capsules were put in an L4514-type diffusion furnace (Qingdao Sunred Electronic Equipment Co., China) at 650 °C, and then heated to the temperatures between 800 and 950 °C depending on the estimated liquidus temperatures of the alloys. After kept at the specific temperatures for 1-2 h, the furnace was slowly cooled down to 500 °C and the capsules were quenched in cold water. All the alloys prepared by the above process were annealed at 500 °C for 60-160 days and then quenched in cold water by breaking the quartz tubes.

The metallographic samples of the alloys were analyzed with an electron probe microanalyzer (EPMA) (JXA-8530F, JEOL, Japan), employing pure Mg (99.99 wt.%), Zn (99.999 wt.%) and Y (99.9 wt.%) as standard materials. The EPMA measurements were performed at 15 kV and 2×10^{-8} A. X-ray diffraction (XRD) was performed on powders of annealed alloys using a Cu Kα radiation on a Rigaku D-max/2550 VB + x-ray diffractometer at 40 kV and 200 mA.

3 Experimental Results

Table 1 summarizes the nominal alloy compositions, identified phases and determined phase equilibrium data. Ternary phases of the Y_5Mg_{24} and YMg_2 are denoted as (Y_5Mg_{24}) and (YMg_2) just like (Mg), as they have large ternary homogeneity ranges. All the chemical compositions in the Tables and in the following text are in atomic percent unless otherwise stated.

Figure 2 and 3 show the XRD patterns and backscattered electron (BSE) images of the representative alloys, respectively. Figure 4(a) presents the isothermal section at 500 °C in the Mg-rich region of < 34 at.% Y and < 50 at.% Zn, which was constructed according to the present work and the currently accepted binary phase diagrams from literature.[11] Figure 4(b) is the enlarged view for the region of above 70 at.% Mg. Figure 5 exhibits the isothermal section at 500 °C below 50 at.% Y, integrating Fig. 1 and 4. Well determined tie-triangles are shown with solid lines while the phase equilibria, which were deduced or not well determined, are indicated with dashed lines. Seven more ternary phases were found in the Mg-rich region at 500 °C in the present work, in addition to the Zn-rich ternary phases (τ_1 to τ_7) determined in our previous work.[9] Among them, the two most Mg-rich ternary phases, i.e. the most well-known 14H and 18R LPSO phases as to be discussed in section 3, are designated as τ_8 and τ_9, respectively. The rest of the ternary phases were subsequently denoted as τ_{10} to τ_{14}, roughly with the Mg content in them decreasing. It should be noted that the 10H phase is involved in the phase equilibria with the Zn-rich phases and had been previously labeled as "τ_8",[9] but now renamed as τ_{13} in the present work. Table 2 summarizes the crystallographic and compositional data of the LPSO structures (24R, 14H, 18R and10H) reported in literature, the presently observed ternary phases in the Mg-rich region and the relevant literature data.

4 Ternary Phases

Seven ternary phases, namely τ_8 to τ_{14}, were determined to exist in the Mg-rich region of less than 25 at.% Y and 20 at.% Zn, as shown in Fig. 4. Six of them, τ_8 to τ_{13}, are very close to one another and located sequentially along a line of Y/Zn ratio $\approx 4/3$. Figure 2(a)-(c) are the XRD patterns of the alloys #1, #3 plus #4, and #8 plus #9, respectively. The diffraction peaks of the $Mg_{12}YZn$ phase with the PDF number of 36-1273 can be indexed from the XRD patterns of the five alloys. The microstructures of the five alloys are displayed in Fig. 3(a), (c), (d), (h) and (i), respectively. The EPMA investigation revealed that five

Table 1 Summary of the experimental information on the phase equilibria in the alloys annealed at 500 °C for 60-160 days

| N^o	Nominal composition[a]			Measured composition[b]					
	Mg	Y	Zn	Phase 1		Phase 2		Phase 3	
			(annealing time)[c]	Y	Zn	Y	Zn	Y	Zn
1^d	88.5	6.5	5.0	τ_8		τ_9		τ_{11}	
			(90 days)	7.2	5.8	8.0	6.5	8.9	7.2
				(Mg)		τ_8			
				1.1	0.6	6.1	4.8		
2	86.5	7.5	6.0	τ_8		τ_9		τ_{11}	
			(160 days)	7.3	5.8	8.2	6.5	9.0	7.3
3	88.7	8.3	3.0	(Y_5Mg_{24})		τ_9		(Mg)	
			(90 days)	12.7	1.4	8.3	5.5	3.5	0.3
4	83.5	10.5	6.0	(Y_5Mg_{24})		τ_9		τ_{12}	
			(160 days)	12.8	1.6	8.8	6.2	10.6	7.5
5	80.7	12.6	6.7	(Y_5Mg_{24})		τ_{12}		τ_{13}	
			(160 days)	13.6	1.9	11.4	8.2	13.0	9.3
6	60.0	12.0	28.0	(Mg)		τ_6		Liq	
			(90 days)	0.0	2.6	25.0	47.7	3.2	25.6
7	85.0	6.0	9.0 (160 days)	(Mg)		τ_8		τ_6	
				0.5	1.0	6.0	5.3	24.8	46.7
8	85.0	8.0	7.0	τ_8		τ_{10}		τ_6	
			(160 days)	7.2	6.4	7.7	6.8	24.8	46.5
9^d	81.5	9.5	9.0	τ_8		τ_{10}		τ_{11}	
			(90 days)	7.3	6.2	7.9	6.7	8.9	7.5
				τ_{10}		τ_{11}		τ_6	
				8.2	7.1	9.1	7.6	24.9	44.7
10	83.0	9.0	8.0	τ_{10}		τ_{11}		τ_6	
			(160 days)	8.3	7.3	9.2	7.7	25.0	46.2
11	80.5	10.5	9.0	τ_{11}		τ_{12}		τ_6	
			(160 days)	9.6	7.7	10.6	8.7	24.8	45.5
12	78.5	12.0	9.5	τ_{12}		τ_{13}		τ_6	
			(60 days)	11.1	8.9	12.7	9.8	24.7	40.8
13	78.5	16.5	5.0	(Y_5Mg_{24})		τ_{13}		τ_{14}	
			(160 days)	15.7	2.3	13.8	9.6	21.7	10.7
14	73.0	20.5	6.5	(Y_5Mg_{24})		(YMg_2)		τ_{14}	
			(160 days)	15.8	2.1	23.5	3.6	22.0	10.7
15	66.5	19.0	14.5	τ_{13}		τ_{14}		τ_7	
			(90 days)	13.7	10.1	22.1	15.6	33.4	32.9
16	53.5	27.5	19.0	(YMg_2)		τ_{14}		τ_7	
			(90 days)	24.3	4.5	22.3	13.8	33.5	32.6

[a] Nominal composition of the alloys (in at.%)

[b] Measured compositions of the phases in the alloys (in at.%, balance: Mg)

[c] Annealing time at 500 °C

[d] Four phases appeared in alloys #1 and #9. And two sets of phase equilibrium data were determined in these two alloys

LPSO phases (τ_8 to τ_{12}) with an approximate Y/Zn ratio of 4:3 (see Table 1) appear stable in the five annealed alloys at 500 °C. Meanwhile, it could be inferred from the XRD results that these phases are closely related in crystal structure and have very similar diffraction patterns. And it is rather difficult to differentiate them from one another with the conventional XRD method. Therefore, we have to rely on the microstructural and equilibrium phase
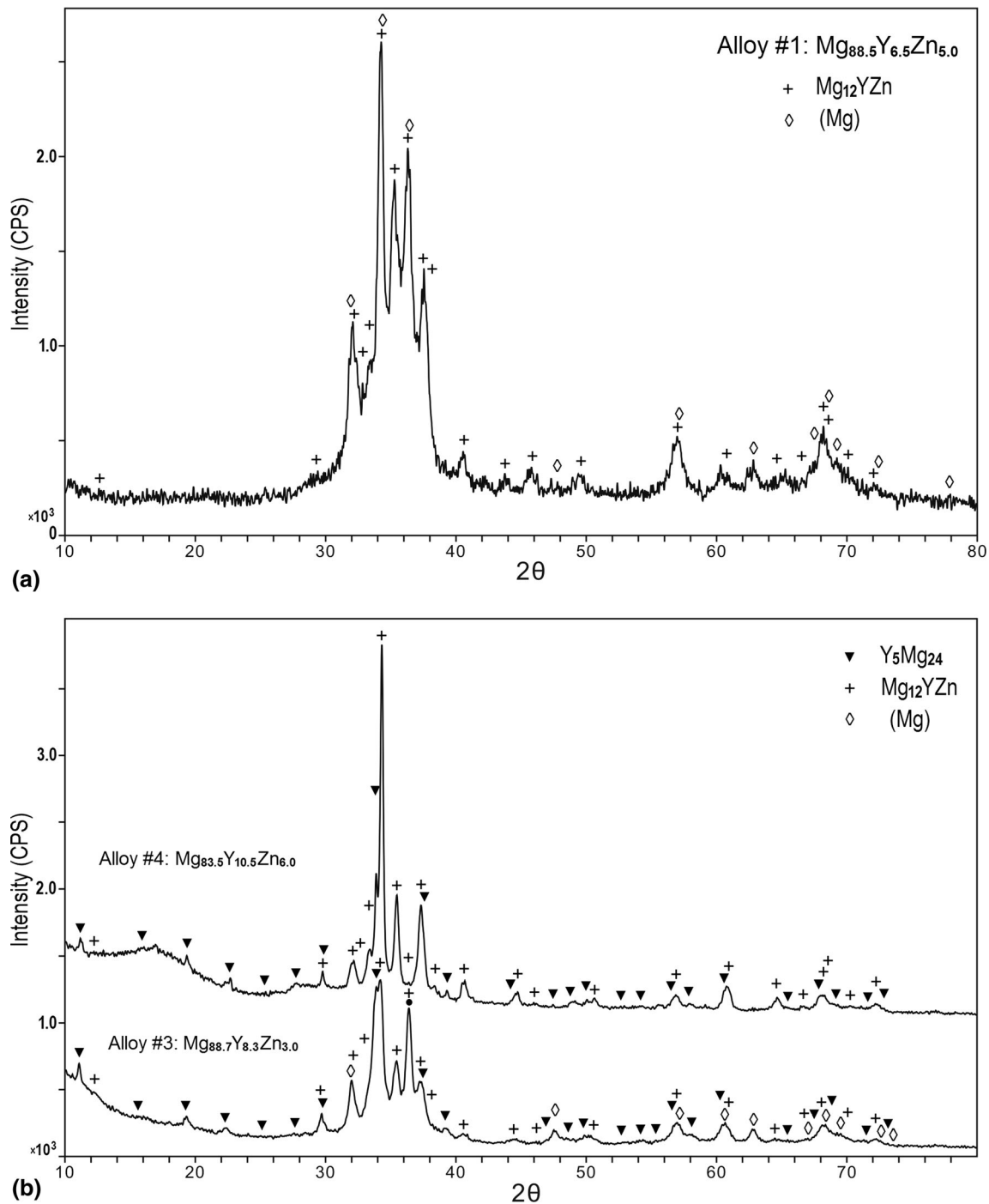
Fig. 2 XRD patterns of alloys (a) alloy #1; (b) alloys #3 and #4; (c) alloys #8 and #9

compositions' examination with EPMA to distinguish these phases and determine the phase equilibria among them.

The $Mg_{12}YZn$ phase, which was called as the X-phase in the literature,[12–14] was considered by some groups of researchers[13,15] to have the 18R-LPSO structure and have a less Zn composition than that of the 14H-LPSO structure.[5] Zhu et al.[16] investigated the Mg-8Y-2Zn-0.6Zr (in wt.%) alloy annealed at 500 °C for 60 h. Their measured

compositions by TEM-EDS are $Mg_{87}Zn_{(6\pm2)}Y_{(7\pm2)}$ for 14H and $Mg_{84}Zn_{(8\pm2)}Y_{(8\pm2)}$ for 18R. Zhu et al.[16] reached a contrary conclusion that the composition formula of the 14H phase is X-$Mg_{12}YZn$ while that of 18R is $Mg_{10}YZn$ rather than the previously accepted $Mg_{12}YZn$. Afterwards, Gong et al.[17] performed neutron diffraction on LPSO Structure in Mg-Zn-Y alloys, and found that an as-cast $Mg_{85}Zn_6Y_9$ alloy produced via high frequency induction
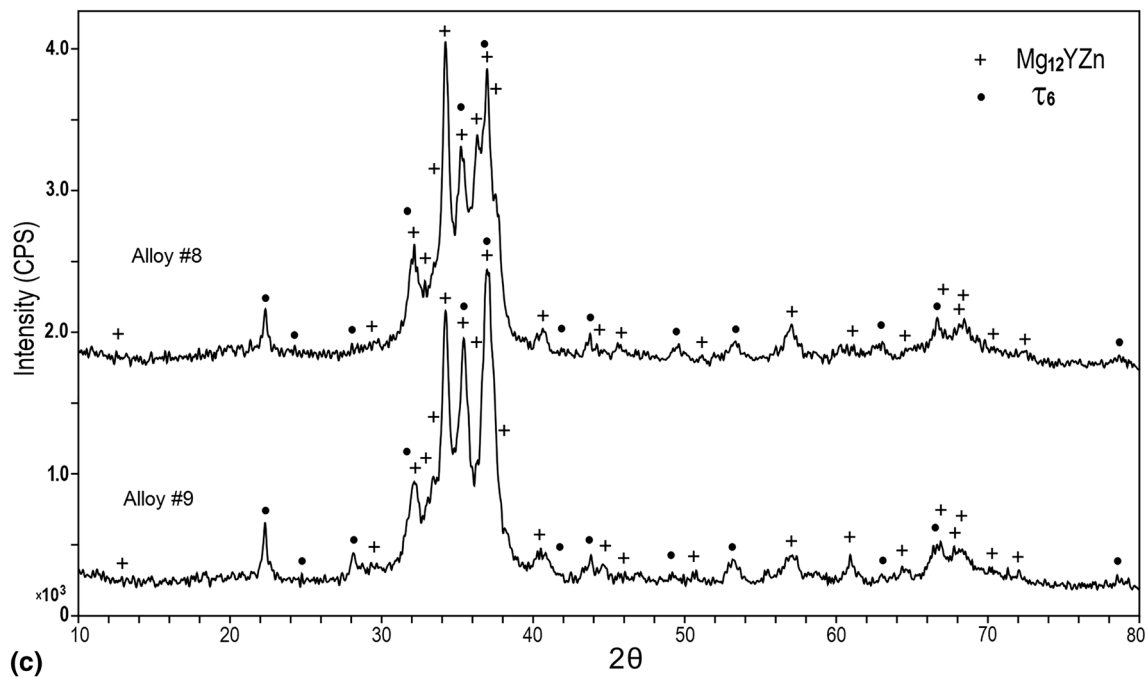
Fig. 2 continued

heating method consists of 18R, together with a small amount of 14H and α-Mg phases. The composition of 14H was measured by Egusa and Abe[7] with EDS-TEM to be $Mg_{94}Zn_{2.0\pm1.0}Y_{4\pm2.0}$. Recently, Kishida et al.[3] investigated the LPSO phases with STEM-EDS in the Mg—8.3 at.% Zn—11.1 at.% Y and Mg—10.0 at.% Zn—13.3 at.% Y alloys, which were annealed at 500 °C for 72 h. Their measured compositions for the 14H and 18R phases are $Mg_{83.5\pm}Zn_{6.7\pm0.2}Y_{9.8\pm0.4}$ and $Mg_{80.5\pm}Zn_{8.4\pm0.4-}Y_{11.1\pm0.2}$, respectively, which are obviously less Mg-rich compared to the reports by Zhu et al.,[16] but closer to the ideal models, i.e. $Mg_{83.33}Zn_{7.14}Y_{9.52}$ ($Mg_{35}Zn_3Y_4$) for 14H and $Mg_{80.56}Zn_{8.33}Y_{11.11}$ ($Mg_{29}Zn_3Y_4$) for 18R.[2] A comprehensive comparison of the measured compositions of the 14H and 18R[3,7,16,17] reveals a fact that 14H has a higher Mg composition than 18R. This conclusion is perhaps more meaningful than a direct usage of the reported compositions in literature, as the reported data by different research groups probably had different errors even though the calibrations had been done.

Generally, the accuracy of the measured compositions for the LPSO phases is largely affected by their size and morphology (i.e. the quality of the examined specimen) as well as the analysis method. Unfortunately, most of the investigated alloys in literature had not been sufficiently annealed to ensure that the analyzed phases grew into sufficient sizes. The accuracy of the measured compositions in such specimen is very likely to be low, due to negative influence from other phases such as the matrix phase. And then likely a measured composition for one

structure could considerably deviate from its real composition.

The compositions of the six ternary phases in the Mg-rich region (see Table 2) were determined in the present work to be $Mg_{86.4-89.1}Zn_{4.8-6.4}Y_{6.0-7.3}$ (τ_8), $Mg_{85.0-86.2}Zn_{5.5-6.5}Y_{8.2-8.8}$ (τ_9), $Mg_{84.4-85.5}Zn_{6.8-7.3}Y_{7.7-8.3}$ (τ_{10}), $Mg_{82.7-83.9}Zn_{7.2-7.7}Y_{8.9-9.6}$ (τ_{11}), $Mg_{80.0-81.9}Zn_{7.5-8.9}Y_{10.6-11.4}$ (τ_{12}), and $Mg_{75.5-77.7}Zn_{9.3-10.8}Y_{12.7-13.8}$ (τ_{13}). Taking into account experimental technique and specimen quality, it is safe to assume that the errors in the EDS measurements[3,7,16] are higher than those in the present EPMA measurements. The τ_8 phase is the most Mg-rich phase (Table 2) and in equilibrium with (Mg). Its composition range is close to the composition of $Mg_{87}Zn_{(6\pm2)}Y_{(7\pm2)}$ (14H).[16] So τ_8 is considered to be $Mg_{12}YZn$ (14H).[3,16] τ_9 with a composition range of $Mg_{85.0-86.2}Zn_{5.5-6.5}Y_{8.2-8.8}$ is expected to be $Mg_{10}YZn$ (18R), as it is in equilibrium with (Mg) and its composition is very close to $Mg_{85}Zn_6Y_9$ (18R).[17]

The presently measured composition range ($Mg_{75.5-77.7}Zn_{9.3-10.8}Y_{12.7-13.8}$) of τ_{13} covers the reported values of the $Mg_{77.22}Zn_{9.68\pm0.03}Y_{13.10\pm0.08}$[2] and $Mg_{76.2-}Zn_{10.5\pm0.4}Y_{13.3\pm0.4}$[3] for 10H, so τ_{13} is believed to be 10H. τ_{14} was determined to have a composition range of $Mg_{62.3-67.6}Zn_{10.7-15.6}Y_{21.7-22.3}$, which covers the given composition $Mg_{63}Zn_{14}Y_{23}$ by Yamasaki et al.[2] for a crystallographically unknown phase.

In summary, the available information in literature on the compositions and thermal stability of the LPSO structures is still very limited. For instance, there is no report on the experimentally measured compositions for the 24R
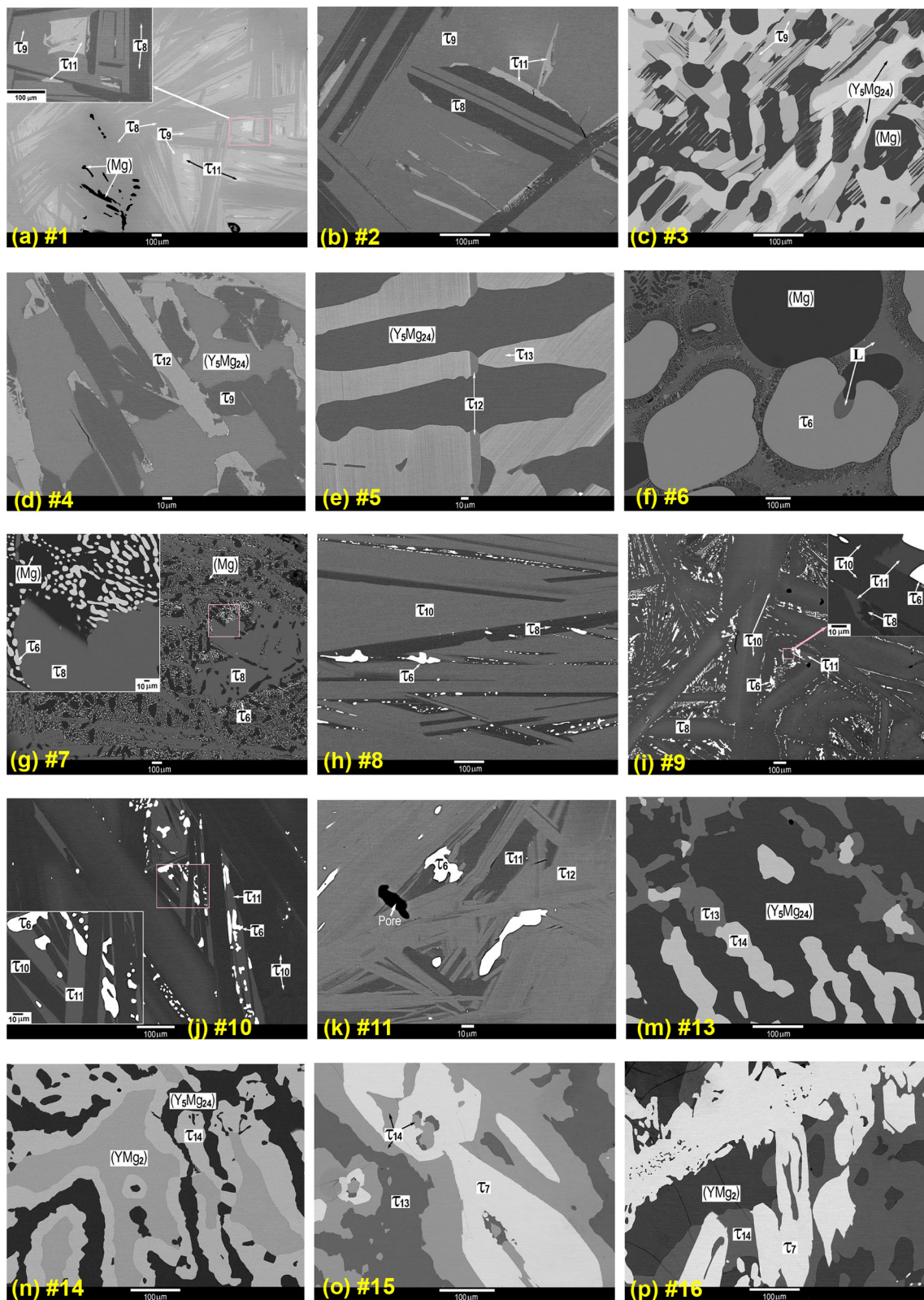
Fig. 3 BSE micrographs of the alloys annealed at 500 °C. (a) alloy #1 (500 °C * 90 days); (b) alloy #2 (500 °C * 160 days); (c) alloy #3 (500 °C * 90 days); (d) alloy #4 (500 °C * 160 days); (e) alloy #5 (500 °C * 160 days); (f) alloy #6 (500 °C * 90 days); (g) alloy #7 (500 °C * 160 days); (h) alloy #8 (500 °C * 160 days); (i) alloy #9 (500 °C * 90 days); (j) alloy #10 (500 °C * 160 days); (k) alloy #11 (500 °C * 160 days); (m) alloy #13 (500 °C * 160 days); (n) alloy #14 (500 °C * 160 days); (o) alloy #15 (500 °C * 90 days); (p) alloy #16 (500 °C * 90 days)

678

J. Phase Equilib. Diffus. (2020) 41:672–680
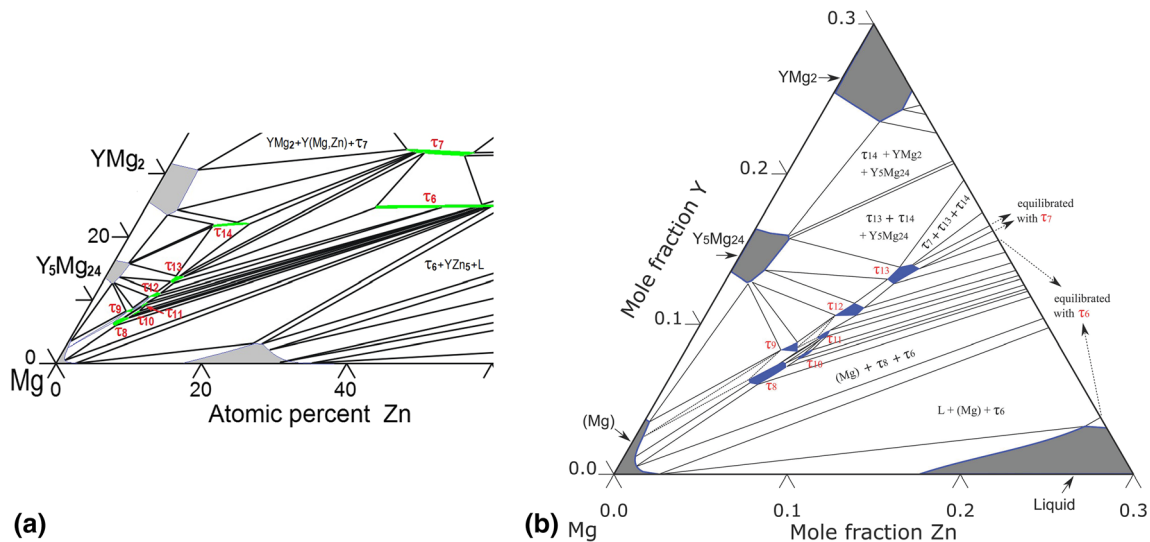
Fig. 4 (a) isothermal section at 500 °C of the Mg-Y-Zn system in the Mg-rich region of < 34 at.% Y and < 50 at.% Zn; (b) Enlarged view of the composition region of above 70 at.% Mg for (a)
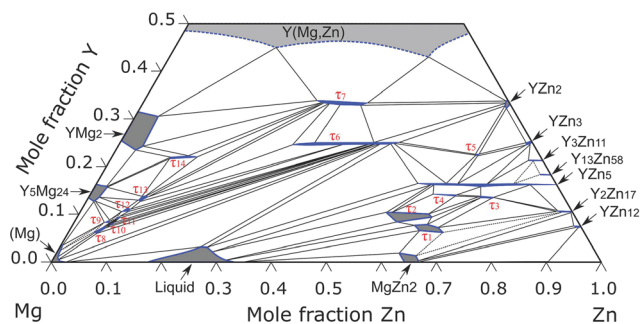
Fig. 5 Isothermal section at 500 °C in the Mg-MgY-YZn-Zn region

structure. Most of the reported compositions for LPSO phases were probably subjected to large errors due to the lack of good specimen. The present work did not aim at a crystallographic analysis of the LPSO phases. Instead, we performed systematic compositional measurements of the phases using a relatively large number of well-annealed alloys, and well determined their phase boundaries and phase relationships.

5 Phase Equilibria

Alloy #1 was mainly composed of the τ_8 phase and contained a small amount of the τ_9 and (Mg) phases as well as a tiny amount of the τ_{11} phase. Figure 3(a) highlights a special view of alloy #1 simultaneously containing the four phases τ_8, τ_9, τ_{11} and (Mg). This indicates that the alloy did not attain full equilibrium even after such a long annealing. Nevertheless, one can still obtain valuable data according to the local equilibrium principle, which is often applied to analyze the phase equilibria in diffusion couples. The inset

at upper left corner is the local magnification of the marked square area. As seen in Fig. 3(a), the dark phase is (Mg) and was scattered within the grey τ_8 phase. The white τ_{11} phase mainly appeared in τ_9, but a portion of it was adjacent to the τ_8/τ_9 boundary. In other words, the three-phase equilibrium of $\tau_8 + \tau_9 + \tau_{11}$, together with a tie-line between τ_8 and (Mg), was determined in this alloy. This three-phase equilibrium was confirmed in alloy #2, as seen in Fig. 3(b).

As revealed by the BSE images in Fig. 3(c) and (d), alloys #3 and #4 are in the three-phase equilibria of $\tau_9 + (Y_5Mg_{24}) + (Mg)$ and of $\tau_9 + (Y_5Mg_{24}) + \tau_{12}$, respectively.

The BSE image of alloy #5 (Fig. 3(e)) clearly shows a three-phase equilibrium, which was determined to be of $(Y_5Mg_{24}) + \tau_{12} + \tau_{13}$. It should be noted that lamellar (thin line-shaped) τ_{12} seemed to be dispersed in the region designated as τ_{13}. Nevertheless, it is still easy to find homogeneous areas made of the single τ_{13} phase and to accurately measure its composition with EPMA. Alloy #6 is in the three-phase equilibrium of $(Mg) + \tau_6 + Liq$ (Table 1). As shown in the BSE image (Fig. 3(f)), the big grains indicate that the annealing is sufficient while the fine microstructures within the region "Liq" obviously formed during the followed quenching. Considering the severe solidification segregation, the average equilibrium composition of the liquid phase at 500 °C (Table 1) was obtained by EPMA measurement of the large solidification areas.

Figure 3(g) and (h) exhibit the BSE images of alloys #7 and #8, respectively. Both τ_8 in alloy #7 and the τ_{10} in alloy #8 had grown to gigantic size after being annealed at 500 °C for up to 160 days. Alloy #7 is in the three-phase

J. Phase Equilib. Diffus. (2020) 41:672–680

679

Table 2 Summary of the ternary phases in the Mg-rich region of the Mg-Y-Zn system

Phase name/composition range	Space group	Lattice parameters, nm	Alternative designation, Reference
24R[a]		$a = 0.322$, $c = 6.181$[6]	$Mg_{41}Zn_3Y_4$[2]
14H[a]	$P6_322$[3]	$a = 0.325$, $c = 3.694$[6]	$Mg_{35}Zn_3Y_4$[2]
			$(Mg_{83.5\pm}Zn_{6.7\pm0.2}Y_{9.8\pm0.4})$[3]
			$(Mg_{87}Zn_7Y_6)$[5]
	$P6_3/mcm$[7]	$a = 1.11$, $c = 3.65$[7]	$(Mg_{94}Zn_{2.0\pm1.0}Y_{4\pm2.0})$[7]
		$a = 1.112$, $c = 3.647$[16]	$Mg_{12}ZnY$ $(Mg_{87\pm}Zn_{6\pm2}Y_{7\pm2})$[16]
18R[a]	$C2/c$[3]	$a = 0.320$, $c = 4.678$[6]	$Mg_{29}Zn_3Y_4$[2]
		$a = 1.5772$, $\alpha = 11.73°$ or	$(Mg_{80.5\pm}Zn_{8.4\pm0.4}Y_{11.1\pm0.2})$[3]
		$a = 0.3224$, $c = 4.6985$[13]	$(Mg_{90}Zn_4Y_6)$[5]
		$a = 0.323$, $c = 4.697$[15]	$X-Mg_{12}ZnY$[13]
		$a = 1.112$, $b = 1.926$	$X-Mg_{12}ZnY$ $(Mg_{85.5}Zn_{7.1}Y_{7.4})$[15]
		$c = 4.689$, $\beta = 83.25°$[16]	$Mg_{10}ZnY$ $(Mg_{84\pm}Zn_{8\pm2}Y_{8\pm2})$[16]
	$P3_212$[17]	$a = 1.1182$, $c = 4.7032$[17]	$(Mg_{85}Zn_6Y_9)$[7,17]
10H[a]	$P6_3/mcm$[2]	$a = 1.11$, $c = 2.60$[2]	$Mg_{23}Y_4Zn_3$ $(Mg_{77.22\pm}Zn_{9.68\pm\ 0.03}Y_{13.1\ \pm\ 0.08})$[2]
	$Cmce$[3]	$a = 0.325$, $c = 2.603$[6]	$(Mg_{76.2\pm}Zn_{10.5\pm0.4}Y_{13.3\pm0.4})$[3]
τ_8[b]			14H, $Mg_{35}Zn_3Y_4$[2]
$Mg_{86.4-89.1}Zn_{4.8-6.4}Y_{6.0-7.3}$			14H/$Mg_{83.5\pm}Zn_{6.7\pm0.2}Y_{9.8\pm0.4}$[3]
			14H/$Mg_{94}Zn_{2.0\pm1.0}Y_{4\pm2.0}$[7]
		$a = 1.112$, $c = 3.647$[16]	14H, $X-Mg_{12}ZnY$/$Mg_{87\pm}Zn_{6\pm2}Y_{7\pm2}$[16]
τ_9[b]		$\boldsymbol{a} = 1.112$, $b = 1.926$	18R, $Mg_{29}Zn_3Y_4$[2]
$Mg_{85.0-86.2}Zn_{5.5-6.5}Y_{8.2-8.8}$		$c = 4.689$, $\beta = 83.25°$[16]	18R, $Mg_{10}ZnY$/$Mg_{84\pm}Zn_{8\pm2}Y_{8\pm2}$[16]
		$a = 1.1182$, $c = 4.7032$[17]	18R/$Mg_{85}Zn_6Y_9$[7,17]
τ_{10}[b]		…[c]	
$Mg_{84.4-85.5}Zn_{6.8-7.3}Y_{7.7-8.3}$			
τ_{11}[b]		…[c]	
$Mg_{82.7-83.9}Zn_{7.2-7.7}Y_{8.9-9.6}$			
τ_{12}[b]		…[c]	
$Mg_{80.0-81.9}Zn_{7.5-8.9}Y_{10.6-11.4}$			
τ_{13}[b]		$a = 1.11$, $c = 2.60$[2]	10H, $Mg_{23}Y_4Zn_3$/$Mg_{77.22\pm}Zn_{9.68\pm\ 0.03}Y_{13.1\ \pm\ 0.08}$[2]
$Mg_{75.5-77.7}Zn_{9.3-10.8}Y_{12.7-13.8}$			10H/$Mg_{76.2\pm}Zn_{10.5\pm0.4}Y_{13.3\pm0.4}$[3]
τ_{14}[b]		…[c]	$Mg_{63}Zn_{14}Y_{23}$[2]
$Mg_{62.3-67.6}Zn_{10.7-15.6}Y_{21.7-22.3}$			

[a]Four types of LPSO structures reported in the literature

[b]Presently observed ternary phases in the Mg-rich region

[c]"…" means "no data available in the literature"

equilibrium of $(Mg) + \tau_6 + \tau_8$ and alloy #8 in $\tau_6 + \tau_8 + \tau_{10}$. The results from the two alloys are self-consistent and the tie-line between τ_8 and τ_6 is confirmed.

Two three-phase equilibria, $\tau_8 + \tau_{10} + \tau_{11}$ and $\tau_6 + \tau_{10} + \tau_{11}$, were detected in alloy #9, as shown in Fig. 3(i). The latter one was corroborated and more accurately determined in alloy #10, as indicated in Fig. 3(j) and listed in Table 1. Actually, both equilibria are in accord with the tie-triangle of $\tau_6 + \tau_8 + \tau_{10}$ determined in alloy #8.

Figure 3(k) displays the BSE images of alloy #11, in which the three-phase equilibrium of $\tau_{11} + \tau_{12} + \tau_6$ was determined. The three-phase equilibrium of $\tau_{12} + \tau_{13} + \tau_6$ was measured on alloy #12, as listed in Table 1.

The τ_{14} phase, which is expected to be identical to the crystallographically unknown $Mg_{63}Zn_{14}Y_{23}$ in Ref 2 as stated in above subsection, was observed in alloys #13-#16. Four three-phase equilibria, i.e. $(Y_5Mg_{24}) + \tau_{13} + \tau_{14}$, $(Y_5Mg_{24}) + (YMg_2) + \tau_{14}$, $\tau_{13} + \tau_{14} + \tau_7$ and $(YMg_2) + \tau_{14} + \tau_7$, were determined in these four alloys, as shown in Fig. 3(m)-(p) and listed in Table 1, respectively.

Gröbner et al.[11] performed a thermodynamic modeling of the Mg-Y-Zn system. Only two LPSO phases (14H and 18R) were taken into account in the Mg-rich region.

Besides, their calculated isothermal section at 500 °C indicated that there is no two-phase field between (Mg) and 18R, and between W-Y$_2$Mg$_3$Zn$_3$ (τ_6) and liquid phase, which does not agree with the present results.

6 Conclusions

The phase equilibria at 500 °C in the Mg-rich region were investigated with 16 equilibrated alloys. A partial isothermal section was constructed for the region of < 34 at.% Y and < 50 at.% Zn using the present results and an extended section of < 50 at.% Y was produced by integrating the data from our previous work.[9]

1. Seven more ternary phases (τ_8 to τ_{14}) were found in the Mg-rich region, in addition to the seven ternary phases (τ_1 to τ_7) previously found in the Zn-rich region.[9] The composition ranges of the ternary phases were determined to be Mg$_{86.4-89.1}$Zn$_{4.8-6.4}$Y$_{6.0-7.3}$ (τ_8), Mg$_{85.0-86.2}$Zn$_{5.5-6.5}$Y$_{8.2-8.8}$ (τ_9), Mg$_{84.4-85.5}$Zn$_{6.8-7.3}$Y$_{7.7-8.3}$ (τ_{10}), Mg$_{82.7-83.9}$Zn$_{7.2-7.7}$Y$_{8.9-9.6}$ (τ_{11}), Mg$_{80.0-81.9}$Zn$_{7.5-8.9}$Y$_{10.6-11.4}$ (τ_{12}), Mg$_{75.5-77.7}$Zn$_{9.3-10.8}$Y$_{12.7-13.8}$ (τ_{13}) and Mg$_{62.3-67.6}$Zn$_{10.7-15.6}$Y$_{21.7-22.3}$ (τ_{14}).

2. The ternary phases τ_8 to τ_{13} are very close in composition and located approximately along the line of Y/Zn ratio = 4/3. They are all believed to have the LPSO structures and closely be related in crystallography. The phases were identified mainly based on systematic compositional measurements and considering their phase relationships. τ_8 is expected to be the X-Mg$_{12}$YZn phase (14H), τ_9 to be the Mg$_{10}$ZnY phase (18R), τ_{13} to be 10H and τ_{14} to be the unknown Mg$_{63}$Zn$_{14}$Y$_{23}$ phase reported by Yamasaki et al.[2]

References

1. J.F. Nie, Y.M. Zhu, and A.J. Morton, On the Structure, Transformation and Deformation of Long-Period Stacking Ordered Phases in Mg-Y-Zn Alloys, *Metall. Mater. Trans. A*, 2014, **45**, p 3338-3348

2. M. Yamasaki, M. Matsushita, K. Hagihara, H. Izuno, E. Abe, and Y. Kawamura, Highly Ordered 10H-Type Long-Period Stacking Order Phase in a Mg-Zn-Y Ternary Alloy, *Scr. Mater.*, 2014, **78–79**, p 13-16

3. K. Kishida, K. Nagai, A. Matsumoto, A. Yasuhara, and H. Inui, Crystal Structures of Highly-Ordered Long-Period Stacking-Ordered Phases with 18R, 14H and 10H-Type Stacking Sequences in the Mg-Zn-Y System, *Acta Mater.*, 2015, **99**, p 228-239

4. J.K. Kim, W.S. Ko, S. Sandlöbes, M. Heidelmann, B. Grabowski, and D. Raabe, The Role of Metastable LPSO Building Block Clusters in Phase Transformations of an Mg-Y-Zn Alloy, *Acta Mater.*, 2016, **112**, p 171-183

5. T. Itoi, T. Seimiya, Y. Kawamura, and M. Hirohash, Long Period Stacking Structures Observed in Mg$_{97}$Zn$_1$Y$_2$ Alloy, *Scr. Mater.*, 2004, **51**, p 107-111

6. M. Matsuda, S. Ii, Y. Kawamura, Y. Ikuhara, and M. Nishida, Variation of Long-Period Stacking Order Structures in Rapidly Solidified Mg$_{97}$Zn$_1$Y$_2$ Alloy, *Mater. Sci. Eng. A*, 2005, **393**, p 269-274

7. D. Egusa and E. Abe, The Structure of Long Period Stacking/ Order Mg-Zn-RE Phases with Extended Non-Stoichiometry Ranges, *Acta Mater.*, 2012, **60**, p 166-178

8. A. Singh, Tailoring Microstructure of Mg-Zn-Y Alloys with Quasicrystal and Related Phases for High Mechanical Strength, *Sci. Technol. Adv. Mater.*, 2014, **15**, p 044803

9. T. Zhou, H.H. Xu, and H.L. Chen, Phase Equilibria of the Mg-Y-Zn System at 500 °C in the Region of < 50 at.% Mg and < 50 at.% Y, *J. Phase Equilib. Diffus.*, 2018, **39**, p 778-788

10. H.H. Xu, J.J. Fan, H.L. Chen, R. Schmid-Fetzer, F. Zhang, Y.B. Wang, Q.N. Gao, and T. Zhou, Experimental Determination of the Phase Equilibria of the Mg-Nd-Zn System at 320 °C, *J. Alloys Compd.*, 2014, **603**, p 100-110

11. J. Gröbner, A. Kozlov, X.Y. Fang, J. Geng, J.F. Nie, and R. Schmid-Fetzer, Phase Equilibria and Transformations in Ternary Mg-Rich Mg-Y-Zn Alloys, *Acta Mater.*, 2012, **60**, p 5948-5962

12. E.M. Padezhnova, E.V. Mel'nik, R.A. Miliyevskiy, T.V. Dobatkina, and V.V. Kinzhibalo, Investigation of the Mg-Zn-Y System, *Russ. Metall.*, 1982, **4**, p 185-188

13. Z.P. Luo and S.Q. Zhang, High-Resolution Electron Microscopy on the X-Mg$_{12}$ZnY Phase in a High Strength Mg-Zn-Zr-Y Magnesium Alloy, *J. Mater. Sci. Lett.*, 2000, **19**, p 813-815

14. T. Horiuchi, A. Ono, K. Yoshioka, T. Watanabe, K. Ohkubo, S. Miura, T. Mohri, and S. Tamura, Liquid-Solid Equilibrium and Intermediate Phase Formation During Solidification in Mg-1.3 at.%Zn-1.7 at.%Y Alloy, *Mater. Trans.*, 2008, **49**(10), p 2247-2253

15. K. Hagihara, N. Yokotani, and Y. Umakoshi, Plastic Deformation Behavior of Mg$_{12}$YZn with 18R Long-Period Stacking Ordered Structure, *Intermetallics*, 2010, **18**, p 267-276

16. Y.M. Zhu, A.J. Morton, and J.F. Nie, The 18R and 14H Long-Period Stacking Ordered Structures in Mg-Y-Zn Alloys, *Acta Mater.*, 2010, **58**, p 2936-2947

17. W. Gong, K. Aizawa, S. Harjo, J. Abe, T. Iwahashi, and T. Kamiyama, Neutron Diffraction on LPSO Structure in Mg-Zn-Y Alloys, *Mater. Trans.*, 2013, **54**(6), p 974-976